

APPENDIX F

ESTIMATING THE EXTENT OF THE OLIGOHALINE ZONE IN THE NORTH FORK OF THE ST. LUCIE RIVER AND ESTUARY UNDER LOW FLOW CONDITIONS

Chenxia Qiu, SFWMD

SUMMARY

The location of the 5-parts per thousand (ppt) isohaline zone in the North Fork of the St. Lucie River and Estuary under steady state conditions is estimated using two methods: a one-dimensional analytical solution and a two-dimensional hydrodynamic Research Management Associates, Inc. (RMA) model. The 5-ppt isohaline zone is traditionally considered to be the transition between the saltier mesohaline and the fresher oligohaline habitats. Its location is used here to define the downstream extent of viable oligohaline habitat under low flow situations. The one-dimensional analytic method is calibrated using salinity data collected at the Kellstadt Bridge (FOS station 1), and flow data collected at the Gordy Road Structure during 1999 and 2000. The two-dimensional RMA model was calibrated at the Roosevelt Bridge, which crosses the St. Lucie Estuary. This calibration is discussed in **Appendix H**. A logarithmic relationship is developed relating the salt intrusion position to the discharge rate. The relationship is similar for both solution methods. This relationship can be used to estimate the extent of the viable oligohaline zone in the riverine portions of the North Fork. Based on recommendations from the expert review of models used to support the development of the St. Lucie River and Estuary minimum flows, additional calibration for the hydrodynamic and salinity models was performed. Results are presented in the addendum to this appendices.

BACKGROUND

This work is conducted as part of the Indian River Lagoon Restoration Feasibility Study (USACE and SFWMD, 2001) and also as part of the effort to establish minimum flow and levels (MFLs) for the St. Lucie Estuary. Protection of a viable oligohaline habitat depends in part on the maintenance of sufficient flows within the riverine reaches of the St. Lucie River watershed. Since most of the riverine portions of the watershed are in the historic North Fork, this paper is limited to North Fork modeling. Previous hydrodynamic modeling (**Appendix H**) within the St. Lucie Estuary focused on periods of moderate to high runoff when the riverine portions of the estuary were fresh. For this reason, previous modeling did not extend into the riverine portions of the estuary.

Minimum flow conditions are associated with droughts and periods of low rainfall. Under low flow conditions, salinity throughout the estuary increases and the oligohaline

area is reduced as higher salinity destroys or displaces oligohaline flora and fauna. This MFL work is directed at estimating the extent of the oligohaline under various low flow conditions. Since flows are relatively stable during low flow periods it is assumed that steady state solutions can adequately predict salinity within the upstream reaches.

This appendix describes two steady state methods for predicting the location of the 5-ppt isohaline zone. The calibration of the analytical method is also described. The methods are applied to two minimum flow scenarios (the end of a 1-in-10 year drought). One MFL situation is North Fork flows under predeveloped (Natural System Model [NSM]) conditions. The other scenarios is flow from today's watershed (1995 Base Case) under the same low rainfall conditions. The equivalent flow-location relationships exist for both the 1995 Base Case and NSM conditions using either the analytical or RMS method. The resulting simple flow-location relationship is being applied elsewhere in the continued development of MFL criteria.

ONE-DIMENSIONAL ANALYTICAL SOLUTION

Basic Equations

The objective of the one-dimensional analytical solution is to calculate the location of the isohaline zone in a tidal driven channel with freshwater discharge. The isohaline zone will have 5-ppt or 10-ppt salinity. The method described below in **Figure F-1** and the equations came from Ippen (1966).

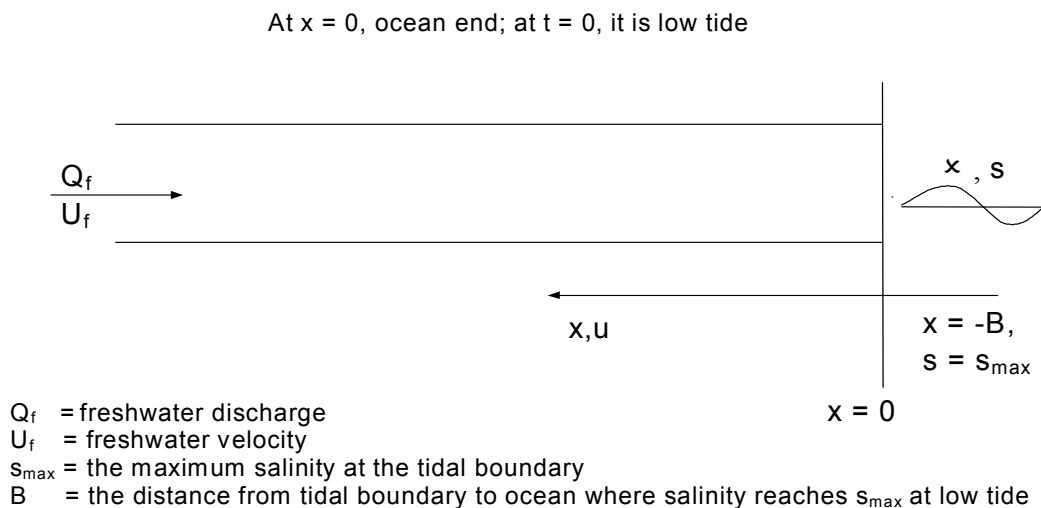


Figure F-1. Sketch of Salinity Intrusion in a Tidal Influenced Channel at Low Tide

Equations 1 and 2 are the basic equations of the one-dimensional analytical solution:

$$\frac{\partial s}{\partial t} + u \frac{\partial s}{\partial x} = \frac{\partial}{\partial x} \left(D_x \frac{\partial s}{\partial x} \right) \quad (1)$$

At any point, the flow velocity in the channel is equal to the sum of the velocity due to tidal motion $u(x,t)$ and the freshwater velocity $-U_f$, thus

$$\frac{\partial s}{\partial t} + u(x,t) \frac{\partial s}{\partial x} - U_f \frac{\partial s}{\partial x} = \frac{\partial}{\partial x} \left(D_x \frac{\partial s}{\partial x} \right) \quad (2)$$

Where $D_x(x,t)$ is the diffusion coefficient.

Solution

Salinity Distribution at Low Tide

The salinity distribution at low tide is determined using Equation 3.

$$\ln \bar{s} + C_2 = -U_f \int \frac{dx}{D_x} \quad (3)$$

Diffusion without Density Difference

The diffusion coefficient can be stated as follows:

$$D_x = 14.2hu \frac{\sqrt{2g}}{C_c} = 7.1hu\sqrt{f}, \quad C_c = \sqrt{8g/f} \quad (4)$$

The average value of D_x in a tidal cycle linearly depends on u , which is computed from tidal propagation and decreases with x in an upstream direction. For uniform cross-sections, a simplest functional relationship can be used:

$$D_x = \frac{D_0 B}{x + B} \quad (5)$$

Therefore,

$$\ln \frac{c}{c_0} = -\frac{U_f}{2BD_0} (x + B)^2 \quad (6)$$

at $x=-B$, $c=c_0$.

Diffusion with Density Difference

The diffusion with density difference is calculated using Equation 7:

$$\ln \frac{s}{s_{\max}} = -\frac{U_f}{2BD_0'}(x_l + B)^2 \quad \text{for } (x_l + B) > 0 \quad (7)$$

The minimum salinity intrusion length at low tide:

$$L_m = x_l = B \left(\sqrt{-\frac{2D_0'}{U_f B} \ln \frac{s}{s_{\max}}} - 1 \right) \quad (8)$$

The maximum salinity intrusion length at high tide is in the range of L_m and L_m+B .

Determine B and D_0'

The distance from the tidal boundary to the ocean where salinity reaches s_{\max} at low tide (B) is determined using Equation 9:

$$B = \frac{u_{\max}}{\sigma} (1 - \cos \sigma t_B) \quad (9)$$

The diffusion coefficient (D_0') is calculated using Equation 10. Because the salinity is in the range of 5 to 15 ppt, assume $D_0' = D_0$

$$D_0' \sim hu_{\max} \frac{\sqrt{2g}}{C_c}, \quad C_c = \frac{1}{n} R^{1/6}, \quad R = \frac{bh}{b+2h} \quad (10)$$

Where t_B is the time the salinity at the entrance reaches the maximum value s_{\max} and s_{\max} is the maximum salinity at low tide at $x_l = 0$. The final D_0' is obtained from calibration. t_B and s_{\max} can be identified from the salinity profile at the ocean end.

Input Parameters

The input parameters for the one-dimensional analytical solution are provided in **Table F-1**.

Table F-1. Input Parameters

Symbol	Parameters	Sources
b	Width	Cross-section profile
h	Depth	Cross-section profile
n	Manning coefficient	
u_{\max}	Maximum velocity at the tidal end boundary	Tidal boundary
s	Tidal frequency	Tidal boundary
U_f	Freshwater velocity	Fresh water discharge Q_f and river cross-section area A
s_{\max}	Maximum salinity at tidal end boundary	Salinity series at tidal boundary
t_B	Time the salinity at the entrance reaches the maximum value s_{\max}	Salinity series at tidal boundary

Implementation Procedures

- Determine σ , u_{\max} , and s_{\max} from the tidal boundary condition
- Determine river depth h and calculate $U_f = Q/A$, where Q is the freshwater discharge rate at cubic meters per second and A is the cross-section area of the river
- Determine t_B and s_{\max} with the salinity series boundary condition
- Calculate B and D_0' from Equations 9 and 10
- Calculate minimum salinity intrusion at low tide with equation (8)

Calibration

The calibration data set is composed of three parts: Florida Oceanographic Society (FOS) Station 1 salinity data (**Figure F-2**), Gordy Road Structure flow data, and Kellstadt Bridge salinity and current data maintained by the United States Geological Survey (USGS) (**Figure F-3**).

Salinity data from FOS Station 1 was taken by volunteers every week since 1998. Station 1 is located 1 mile north of the Prima Vista Bridge (section N044) and 4 to 5 miles north of the Kellstadt Bridge (section N067) (Longitude 80° 19.887' W, Latitude 27° 19.724' N).

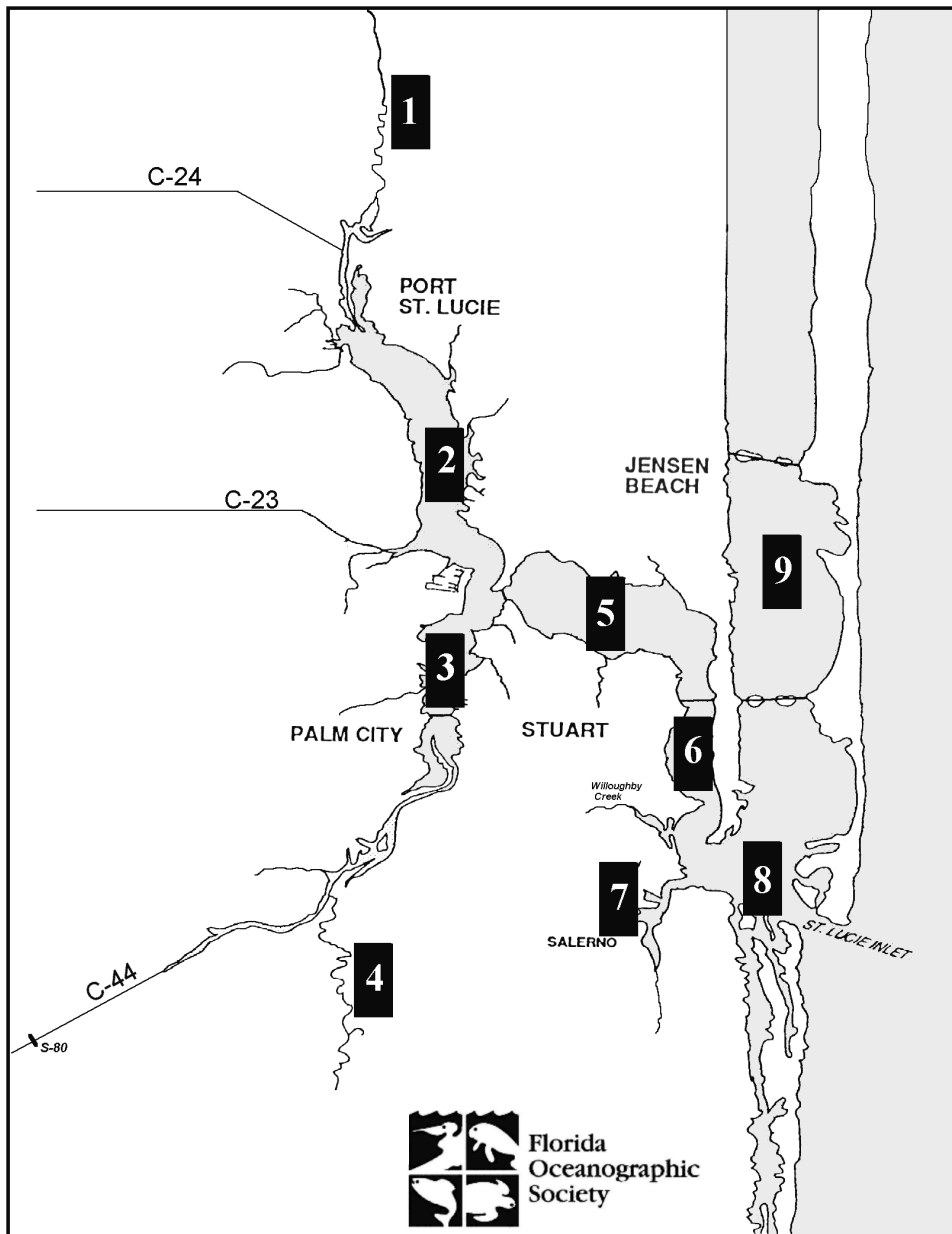


Figure F-2. Florida Oceanographic Society Monitoring Stations

The Kellstadt Bridge station was monitored by USGS until 2000. The monitoring data collected includes water surface elevation, current, and salinity at the top and bottom layers.

The discharge rate at the Gordy Road Structure on Ten Mile Creek has been monitored since 1999. The discharge rate on the North Fork is estimated based on drainage area (**Table F-2**). The approximation in North Fork discharge estimation is probably one of the greatest error terms in this simulation.

Table F-2. North Fork Discharge Derived from Gordy Road Structure Discharge

Drainage Basins	Drainage Area (Acres)
Ten Mile Creek	29,380
Five Mile Creek	7,000
North Fork - Total	105,613
North Fork - uncontrolled area flowing into North Fork	63333
$Q_{NF} = Q_{TMC} * (1 + 63,333/29,380) = Q_{TMC} * 3.16$ Q_{NF} is the total discharge on the North Fork and Q_{TMC} is the discharge on Ten Mile Creek measured at the Gordy Road Structure	

Based on 22 cross-section profiles, it was determined that the North Fork is deeper and wider (230 feet) and meanders down from the Prima Vista Bridge (N035-N072). From Prima Vista Bridge to the upper reach (N01-N035), the river is narrower (85 feet) and shallower. During calibration, the width is fixed constant to 6.5 feet between FOS Station 1 and Kellstadt Bridge. Three calibration scenarios were selected based on the comparison of overlap periods among these 3 data sets (**Table F-3**).

Table F-3. Calibration Scenarios

Calibration scenarios	March 19, 2000	January 23, 2000	December 19, 1999
Freshwater discharge (Q_f) (cubic feet per second)	90	180	260.9
Kellstadt Bridge salinity (ppt)	12	8	3
Salinity at FOS station 1 (north of Prima Vista Bridge) (ppt)	4	2	1.2
Maximum Tidal velocity (u_{max}) (meters per second)	0.3	0.3	0.2
Maximum salinity at tidal end (ppt)	14.8	10.2	5
Minimum salinity at tidal end (ppt)	11	5	1.5
Width (d) (feet)	230		
Depth (h) (feet)	6.5		
Length (mile)	6.4		
Manning coefficient	0.04		
t_B	0.45 Tidal Period		

The diffusion coefficient is crucial for salinity intrusion due to tidal mixing and density gradient. The density gradient effect is reflected in freshwater discharges and salinity at the tidal end. To account for this, the diffusion coefficient is adjusted with a correction factor in the prediction:

$$D'_0 = D_0 \cdot f(Q_f) \cdot f\left(\frac{s_{max}}{s_{min}}\right) = D_0 \cdot \frac{Q_f(\text{calibration base})}{Q_f} \cdot \frac{\ln\left(\frac{s_{max}}{s_{min}}\right)(\text{calibration base})}{\ln\left(\frac{s_{max}}{s_{min}}\right)} \quad (11)$$

Analytical solution is limited with uniform sections. Therefore, average depth is adjusted to 5 feet at low flow conditions based on the two-dimensional simulation results, which is described in the next section.

With the progress of the tide into the river, the velocity amplitude is damped exponentially. In addition, the celerity of wave is reduced by a factor related to wave length. This factor is 0.71 to 0.94 (Ippen, 1966). A conservative correction factor of 0.9 is used.

The one-dimensional analytical solution is limited with simplifications. Through the calibration and prediction process, river depth, river width, maximum salinity, and velocity at the tidal boundary are identified as sensitivity parameters. River depth and width are simplified as uniform. The measured velocity at the Kellstadt Bridge by the USGS is used in the prediction. In addition, the diffusion coefficient is assumed linearly decreased with the propagation of tide. All these approximations introduce uncertainty into the prediction and reflect the limitation of the method.

TWO-DIMENSIONAL SIMULATION ON EXTENDED ESTUARY GRIDS WITH THE RMA MODEL

The RMA finite element grid was extended from Kellstadt Bridge to the Gordy Road Structure. The new grid is shown in **Figure F-3**. The two-dimensional RMA model is calibrated around the Roosevelt Bridge in the St. Lucie Estuary by Hu (**Appendix H**). Due to time limitations, it was not further calibrated for the North Fork.

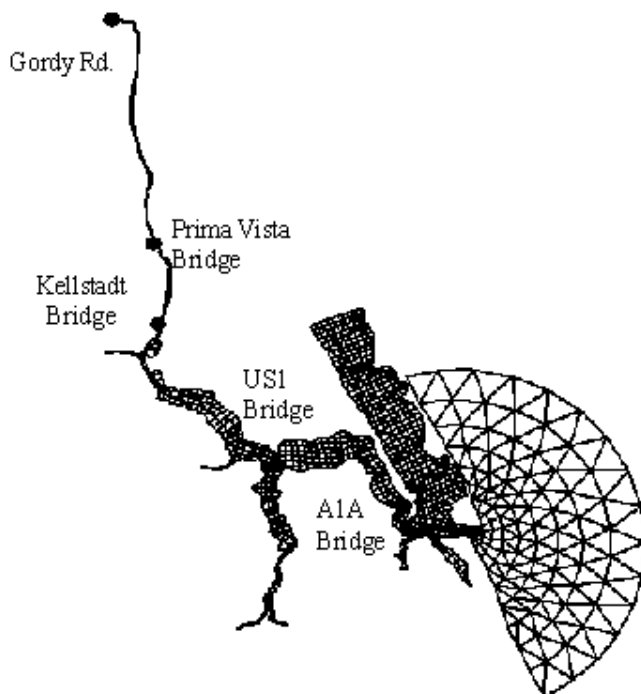


Figure F-3. Two-Dimensional Simulation Grid for the North Fork and the St. Lucie Estuary

RESULTS

Prediction scenarios were selected for 1995 Base Case and NSM model simulations based on the time periods when discharge is relatively stable. Five scenarios were selected for the 1995 Base Case simulations (**Figure F-4** and **Table F-4**) and four were selected for the NSM simulations (**Figure F-5** and **Table F-5**).

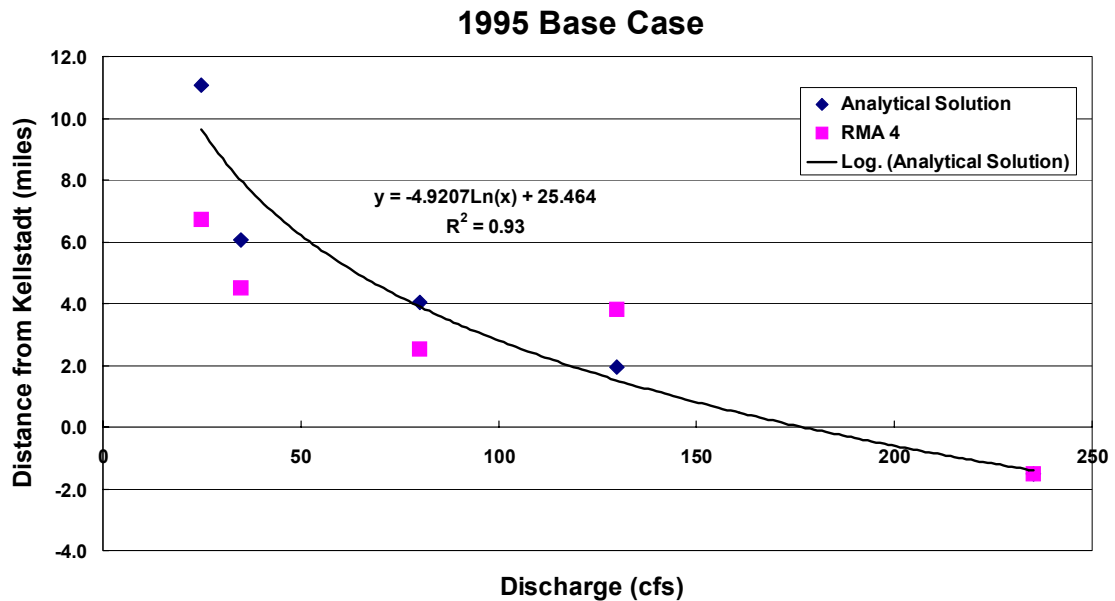


Figure F-4. Location of the 5-ppt Isohaline Zone for the 1995 Base Case Simulations

Table F-4. Prediction Scenarios for the 1995 Base Case

Julian Day	27-42	95-105	19-24	74-79	112-117
Q_f (cfs)	235	130	80	35	25
s_{max}		9.5	13	15	18
s_{min}		6	9	10.5	13
s_{avg}	3.8	8.5	11	12.5	15
L_{avg} (mile) from Kellstadt Bridge	0	2	3	6	11
% of NF length	0	0.14	0.22	0.3	0.5
L_{avg} compared to RMA 4 result	0	5.3	4.0	6.0	8.2
% of NF length	0	0.21	0.16	0.24	0.33

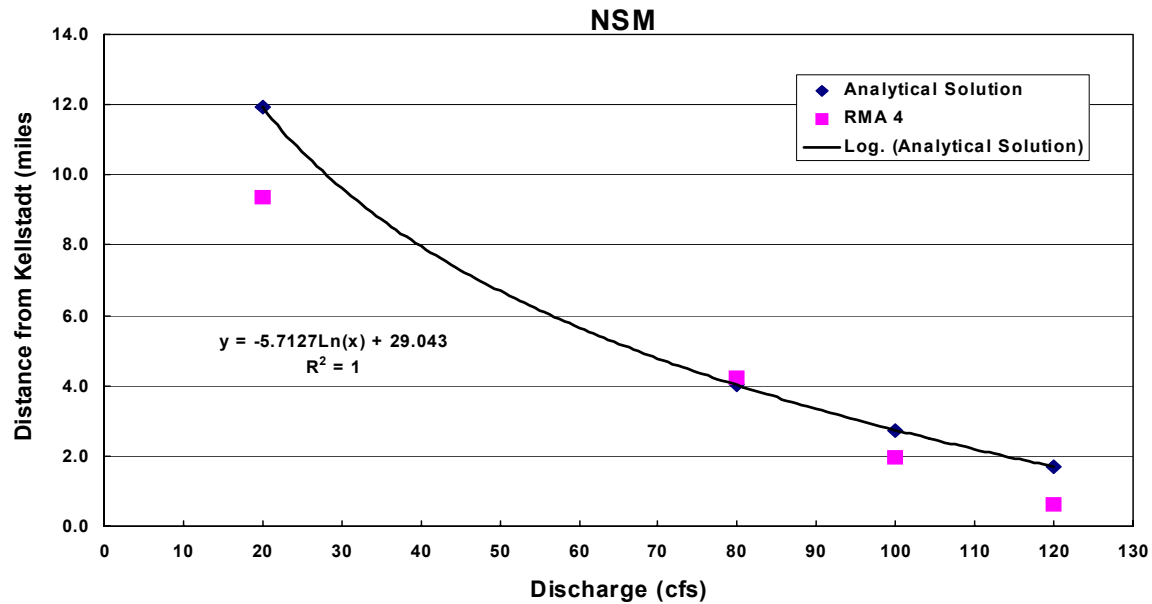


Figure F-5. Location of the 5-ppt Isohaline Zone for the NSM Simulations

Table F-5. Prediction Scenarios for the NSM Simulations

Julian Day	112-119	10-30	52-60	34-50
Q_f (cfs)	20	80	100	120
s_{max}	17.5	14	14	10
s_{min}	14	9	8	6.5
s_{avg}	16	11	10	8
L_{avg} (mile) from the Kellstadt Bridge	12	4	2.7	1.7
% of NF length	0.54	0.22	0.17	0.13
L_{avg} compared to RMA 4 result	10.9	5.7	3.4	2.1
% of NF length	0.43	0.23	0.14	0.08

Based on the results from the two methods, the location of 5-ppt isohaline zone and discharge rate has these relationships:

$$L = -4.9 \ln(Q_f) + 27 \text{ for the 1995 Base Case}$$

$$L = -5.7 \ln(Q_f) + 30.5 \text{ for the NSM}$$

When discharge is larger than 175 cfs for the 1995 Base Case, the 5-ppt isohaline zone is downstream of the Kellstadt Bridge on the North Fork.

CONCLUSION

Predictions of the location of the isohaline zone on the North Fork is conducted with simplifications for a quick solution. Compared with Kellstadt Bridge salinity data from USGS, it is concluded that RMA results underestimated the salt intrusion length on the North Fork, while the one-dimensional analytical solution result is limited by too many simplifications. Due to the limitation of time, the accuracy of the result is compromised.

This simulation will be applied to the determination of the oligohaline zone on the North Fork under minimum flow condition for three scenarios: 1995 Base Case, NSM, and 2050.

REFERENCES

- Florida Oceanographic Society. 2000. *St. Lucie River Estuary Water Quality Outlook*. [http://www.fosusa.org/St. Lucie Estuary.htm](http://www.fosusa.org/St.LucieEstuary.htm).
- Ippen, A.T. 1966. *Estuary and Coastline Hydrodynamics*. McGraw-Hill Book Company, Inc.
- Kjerfve, B. 1978. *Estuarine Transport Processes*. University of South Carolina Press, Columbia, SC.
- McDowell, D.M., and B.A. O'Connor. 1977. *Hydraulic Behavior of Estuaries*. John Wiley & Sons, New York, NY.
- USACE and SFWMD. 2001. *Central and Southern Florida Project, Indian River Lagoon South Feasibility Study, Draft Integrated Feasibility Report and Supplemental Environmental Impact Statement*. Jacksonville District, United States Army Corps of Engineers Jacksonville, FL, and South Florida Water Management District, West Palm Beach, FL.

ADDENDUM TO APPENDIX F

Hydrodynamic and Salinity Model Recalibration for the North Fork of the St. Lucie River

Calibration Data Set

Further calibration of the hydrodynamic and salinity model was conducted with a calibration data set. This data was collected during a 2.5-month period from September 1999 to December 1999. Water level was measured every 15 minutes at the St. Lucie Inlet by the Florida Department Environmental Protection (FDEP). Salinity and water level were measured at the A1A, Roosevelt, and Kellstadt Bridges. Velocity also was measured at the Kellstadt Bridge. Daily flow data was collected at the Gordy Road Structure on Ten Mile Creek. Discharge rates were determined for the C-23, C-24, and C-44 Canals, and the South Fork.

The discharge rate on the North Fork was estimated based on the Gordy Road Structure discharge rate and drainage area. This approximation still contributes the greatest error term in this simulation.

Inlet water level data provides a control at the tidal boundary. It is compared to the 1998 calibration work. This calibration work used the National Ocean and Atmospheric Administration (NOAA) tide book data as its boundary condition.

Simulation Grids and Calibration Stations

The original finite element grids were modified to reflect the meandering of the North Fork. The locations of the FDEP monitoring station at the inlet and the United States Geological Survey (USGS) stations at the A1A, Roosevelt, and Kellstadt Bridges are shown in **Figure F-6**.

Calibration Results

The simulation results of water surface elevation are compared with monitoring data from four stations (**Figures F-7 through F-10**). The salinity calibration results at the A1A, Roosevelt, and Kellstadt Bridges are presented in **Figures F-11 through F-13**.

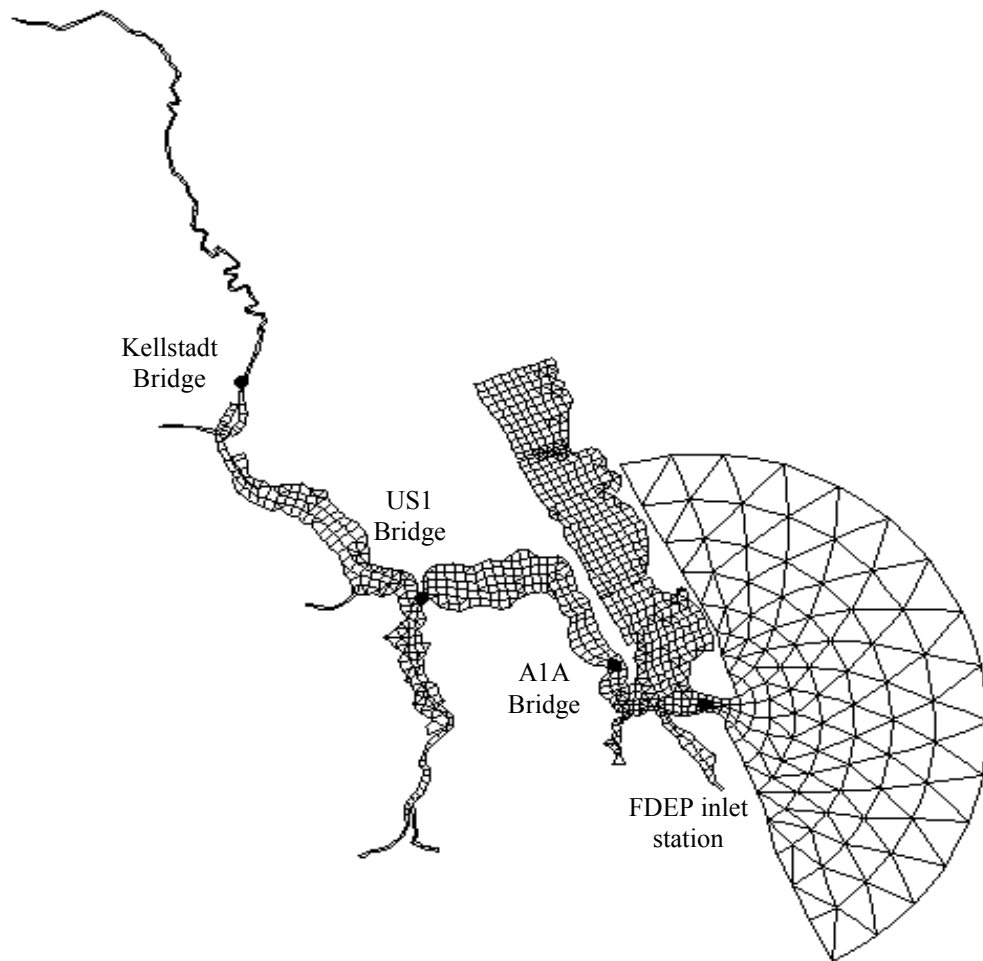


Figure F-6. Simulation Grids and the Locations of Monitoring Stations

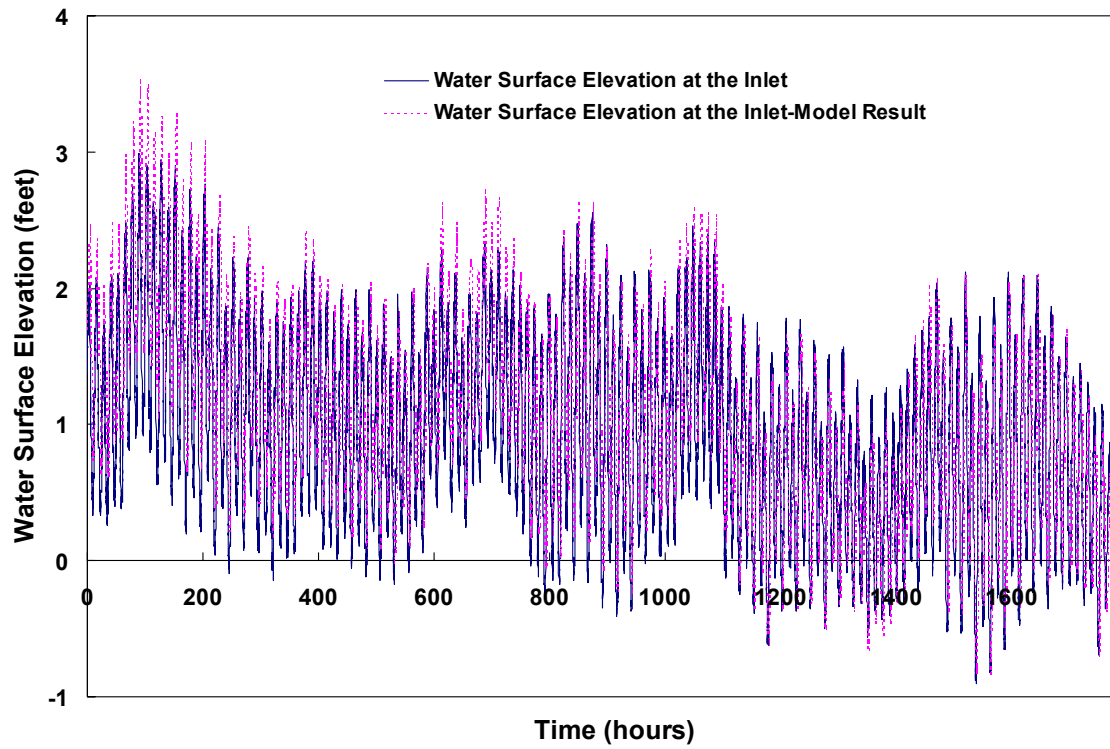


Figure F-7. Water Surface Elevation at the Inlet

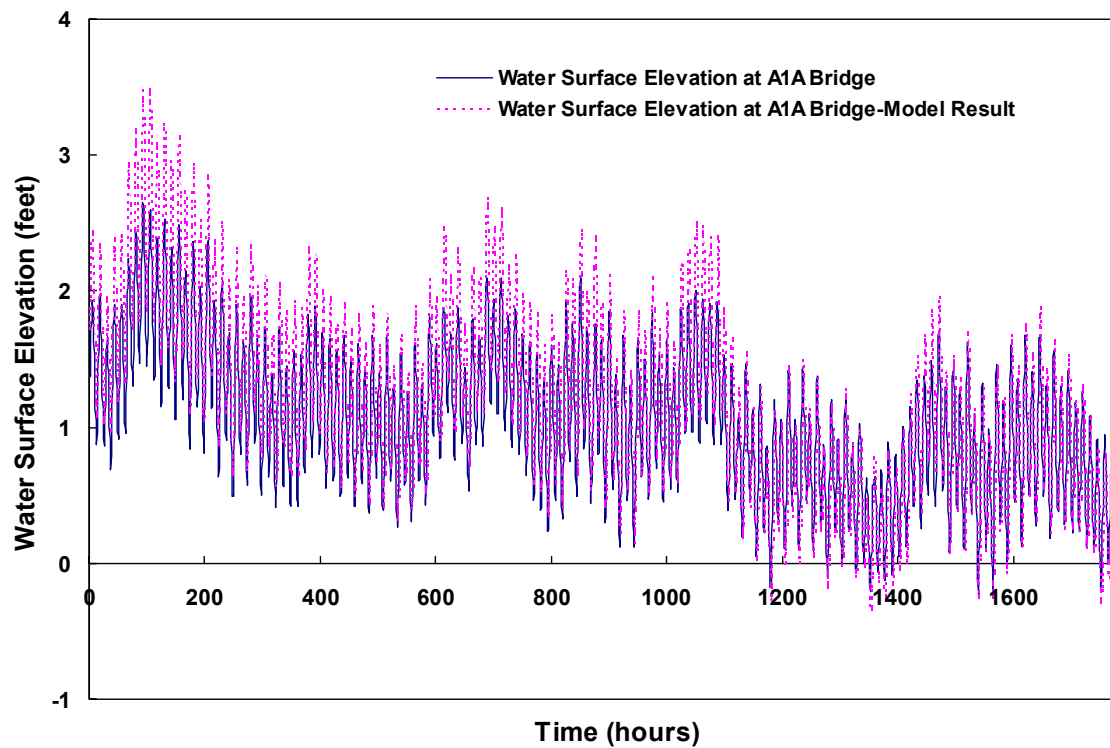


Figure F-8. Water Surface Elevation at the A1A Bridge

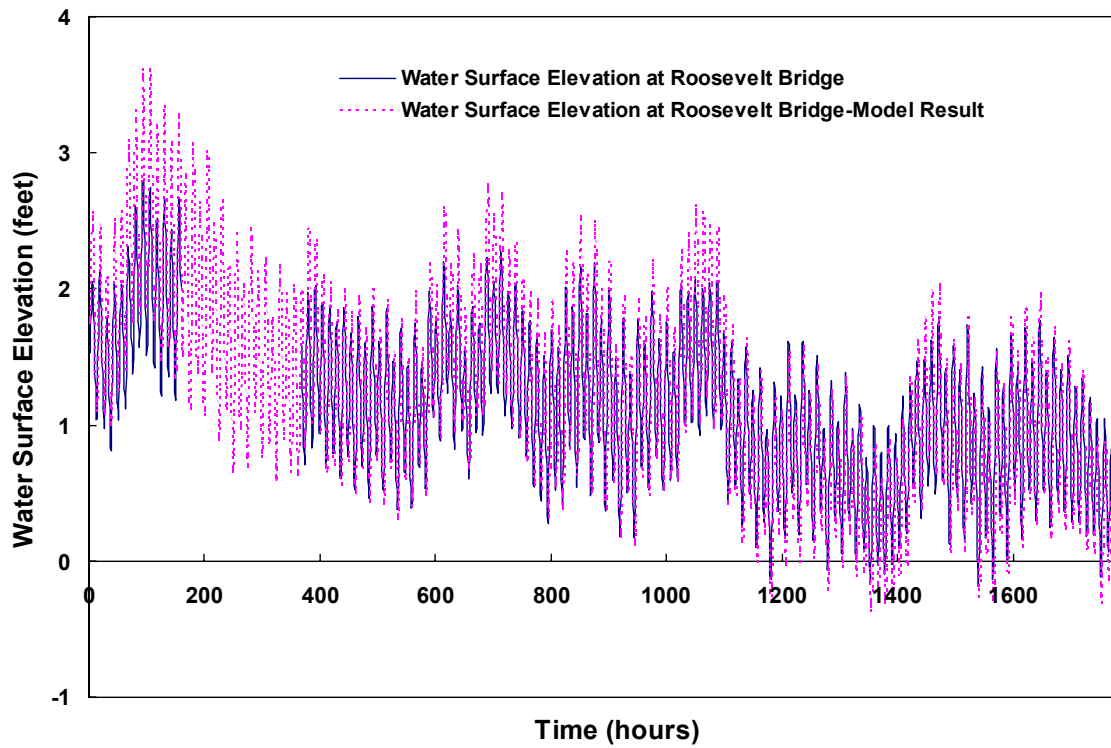


Figure F-9. Water Surface Elevation at the Roosevelt Bridge

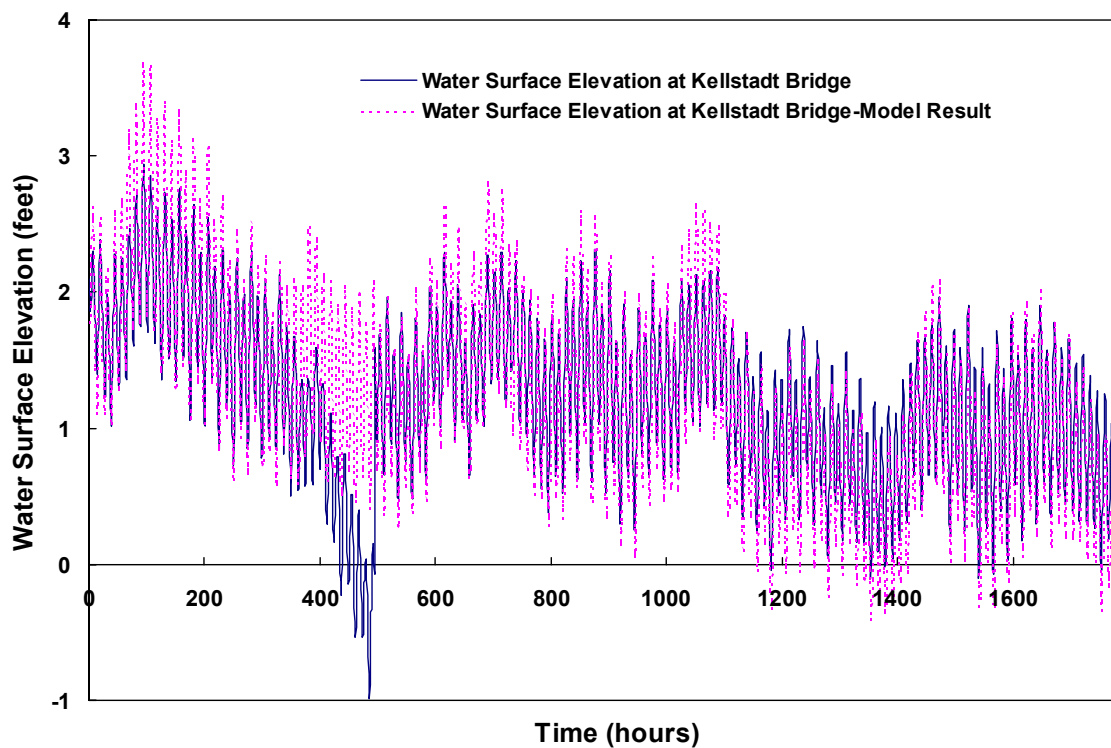


Figure F-10. Water Surface Elevation at the Kellstadt Bridge

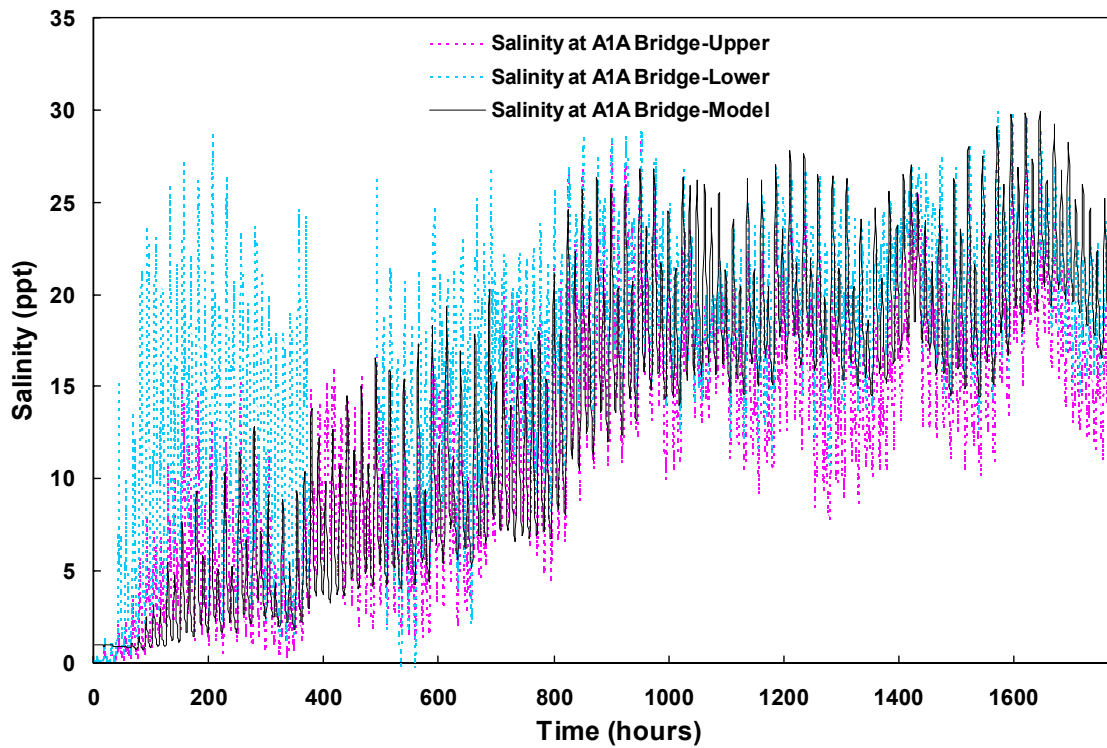


Figure F-11. Salinity at the A1A Bridge

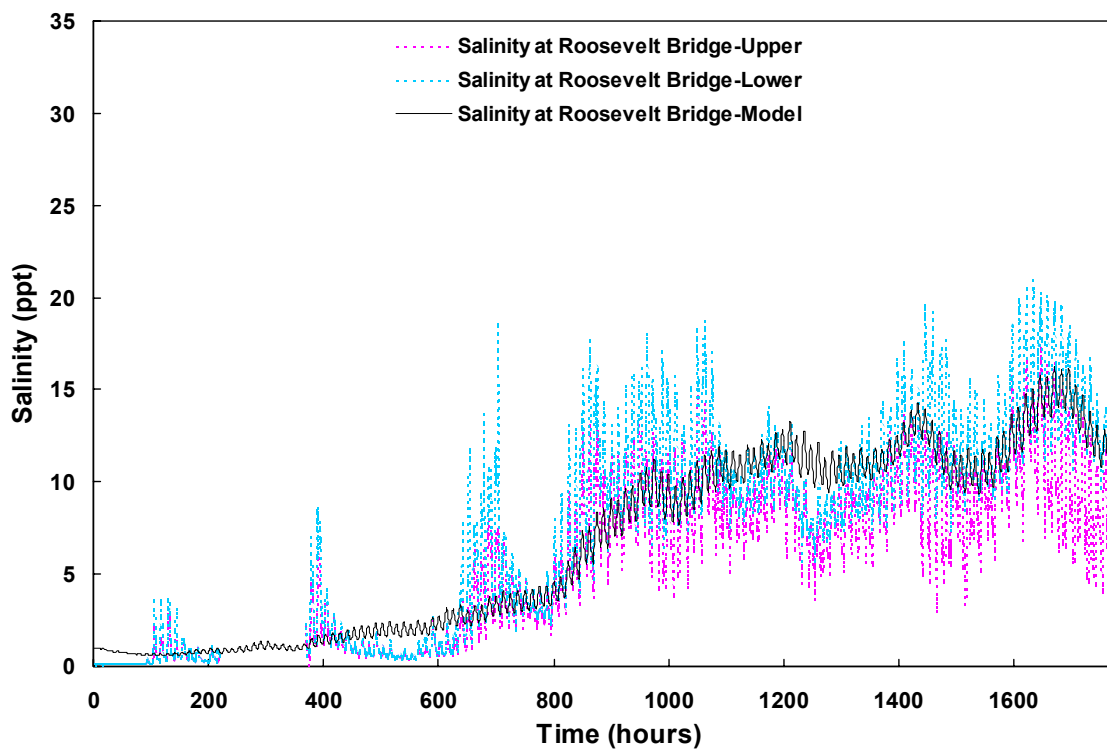


Figure F-12. Salinity at the Roosevelt Bridge

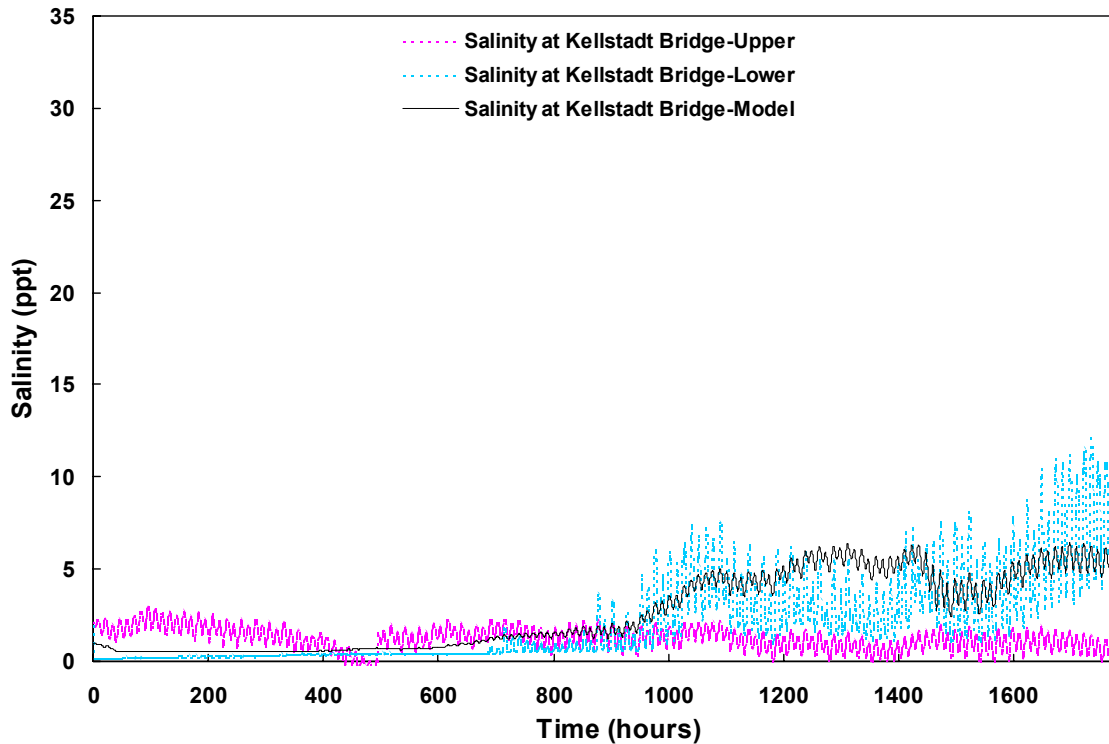


Figure F-13. Salinity at the Kellstadt Bridge

To evaluate the goodness-of-fit between model results and salinity data, the relative errors are calculated based on a daily average. The daily average was used because the discharge rates from inflow canals were measured daily. The calculation formula is as follows:

$$\text{relative error} = \frac{\text{daily averaged salinity result} - \text{daily averaged measurement value}}{\text{maximum of daily measurement value} - \text{minimum of daily measurement value}}$$

The relative errors are shown in **Table F-6**. The first 15 days are excluded to eliminate initial condition effects. Relative errors at the Roosevelt and A1A Bridges are normally in the range of 10 to 20 percent. At Kellstadt Bridge, the majority of relative errors are in the range of 10 to 20 percent except those between day 49 to 60. This might be caused by the inaccurate flow data from the North Fork during that period. In addition, a significant difference between the salinity monitoring data at the top and bottom layers was observed, indicating strong stratification (**Figure F-13**). Although simulation results fall in the middle of salinity data at the top and bottom layers, a three-dimensional model with fine bathymetry data on the North Fork will perform better than a two-dimensional model.

Table F-6. Relative Errors between Simulated Results and Monitored Data

Day	A1A Bridge			Roosevelt Bridge			Kellstadt Bridge		
	Model	Monitored	Relative Error	Model	Monitored	Relative Error	Model	Monitored	Relative Error
16	6.3	9.0	-0.16	1.1	2.3	-0.08	0.5	0.4	0.02
17	6.4	9.4	-0.19	1.4	3.3	-0.14	0.6	0.4	0.03
18	6.4	9.7	-0.20	1.5	1.7	-0.01	0.6	0.4	0.03
19	7.4	8.2	-0.05	1.7	1.1	0.04	0.6	0.4	0.04
20	7.6	7.1	0.03	1.8	0.9	0.07	0.7	0.4	0.04
21	8.0	11.0	-0.19	1.9	0.9	0.07	0.7	0.4	0.04
22	7.6	9.7	-0.12	2.0	0.7	0.09	0.7	0.4	0.04
23	7.4	7.4	0.00	2.0	0.5	0.10	0.7	0.5	0.04
24	8.1	7.7	0.02	2.0	0.7	0.09	0.7	0.5	0.04
25	8.8	11.0	-0.13	2.2	1.1	0.08	0.7	0.5	0.04
26	10.0	12.6	-0.16	2.5	1.1	0.10	0.8	0.4	0.06
27	9.2	10.4	-0.08	2.7	2.0	0.05	0.9	0.5	0.07
28	9.1	9.7	-0.04	2.7	3.9	-0.09	1.0	0.5	0.08
29	11.3	13.6	-0.14	3.0	5.9	-0.20	1.2	0.5	0.11
30	11.0	15.0	-0.24	3.4	6.0	-0.19	1.3	0.8	0.08
31	10.1	15.5	-0.33	3.5	4.0	-0.04	1.3	0.8	0.09
32	10.4	14.4	-0.25	3.6	3.3	0.02	1.4	0.7	0.11
33	10.6	13.4	-0.17	3.7	3.2	0.04	1.5	0.7	0.13
34	12.3	14.8	-0.16	4.1	4.7	-0.04	1.5	0.6	0.13
35	15.5	18.4	-0.18	5.0	6.7	-0.12	1.6	0.7	0.13
36	16.5	19.3	-0.17	6.2	9.2	-0.21	1.6	0.8	0.14
37	17.2	19.0	-0.11	7.1	9.9	-0.20	1.6	1.3	0.05
38	17.1	20.6	-0.22	7.8	9.3	-0.11	1.7	1.3	0.06
39	17.4	20.2	-0.17	8.4	9.7	-0.09	1.8	1.1	0.11
40	18.5	20.1	-0.10	9.2	10.7	-0.11	2.1	1.4	0.11
41	19.5	20.3	-0.05	9.8	10.5	-0.05	2.7	2.7	0.00
42	18.1	17.9	0.01	9.2	9.8	-0.04	3.0	2.8	0.04
43	18.6	18.1	0.03	8.9	10.0	-0.08	3.5	3.5	0.00
44	20.3	18.3	0.12	9.7	10.4	-0.05	4.2	4.6	-0.06
45	20.0	17.0	0.18	10.4	12.0	-0.11	4.5	4.6	-0.01
46	19.1	18.7	0.02	10.8	9.8	0.07	4.6	4.4	0.03
47	18.0	16.9	0.07	10.7	8.8	0.14	4.2	3.2	0.16
48	19.0	17.2	0.11	11.0	8.9	0.15	4.3	3.1	0.19
49	18.9	16.4	0.16	11.3	9.8	0.11	4.4	2.7	0.26
50	19.9	18.0	0.12	11.8	10.4	0.09	4.4	2.7	0.28
51	20.5	20.1	0.02	12.0	9.4	0.18	5.0	3.5	0.25
52	20.2	19.3	0.05	11.3	7.6	0.26	5.4	3.4	0.31
53	19.2	16.8	0.15	10.8	7.0	0.26	5.6	3.1	0.42
54	18.8	15.8	0.19	10.5	8.0	0.18	5.6	2.6	0.48
55	19.0	17.4	0.10	10.8	8.8	0.14	5.8	2.9	0.47
56	18.1	16.0	0.13	10.9	8.9	0.14	5.6	2.5	0.48
57	17.8	16.6	0.07	10.9	9.2	0.13	5.1	2.1	0.48
58	18.7	18.1	0.04	11.4	10.2	0.08	5.1	2.3	0.45
59	20.5	20.4	0.01	12.2	11.5	0.05	5.4	3.0	0.39
60	21.6	23.4	-0.11	13.2	11.4	0.13	5.8	3.8	0.32
61	19.2	20.2	-0.07	12.8	11.7	0.08	4.8	4.0	0.14

Table F-6. Relative Errors between Simulated Results and Monitored Data (Continued)

Day	A1A Bridge			Roosevelt Bridge			Kellstadt Bridge		
	Model	Monitored	Relative Error	Model	Monitored	Relative Error	Model	Monitored	Relative Error
62	18.3	18.4	-0.01	11.4	10.8	0.04	3.7	3.5	0.03
63	19.1	18.3	0.05	10.6	10.1	0.03	3.6	3.2	0.06
64	19.6	19.0	0.04	10.6	9.9	0.05	3.8	3.6	0.03
65	19.4	18.3	0.07	10.6	10.0	0.05	3.5	2.9	0.10
66	21.1	20.2	0.06	11.2	10.7	0.04	4.0	3.1	0.14
67	22.4	21.6	0.05	12.2	12.5	-0.02	4.6	3.7	0.14
68	23.0	21.8	0.07	13.2	13.6	-0.03	5.0	4.1	0.14
69	23.6	22.1	0.09	14.3	14.6	-0.03	5.4	5.0	0.06
70	23.2	20.7	0.15	14.9	13.7	0.08	5.5	5.6	-0.02
71	23.0	18.9	0.25	15.0	12.7	0.16	5.7	6.2	-0.09
72	21.6	17.3	0.26	13.7	12.0	0.13	5.6	6.3	-0.11
73	19.9	17.2	0.16	12.3	10.8	0.11	5.5	6.6	-0.18
74	19.2	17.4	0.11	11.6	10.3	0.10	5.4	6.4	-0.16
Average	16.1	16.3	-0.03	8.2	7.8	0.06	3.2	2.4	0.17

Application to the MFL Salinity Simulation

Based on the time periods when discharge was relatively stable, five prediction scenarios were selected for the 1995 Base Case and four were selected for the NSM. **Table F-7** and **Figure F-14** present the prediction scenarios for the 1995 Base Case. **Table F-8** and **Figure F-15** present the prediction scenarios for the NSM.

Table F-7. Prediction Scenarios Selected for the 1995 Base Case

Julian Day	27-42	95-105	19-24	74-79	112-117
Discharge (cfs)	235	130	80	35	25
Miles Upstream from Kellstadt Bridge	-1.5	2.5	3.5	10.5	13.4

Table F-8. Prediction Scenarios Selected for the NSM

Julian Day	34-50	52-60	10-30	112-119	34-50
Discharge (cfs)	120	100	80	20	120
Miles Upstream from Kellstadt Bridge	0	0.5	4.5	13.5	0

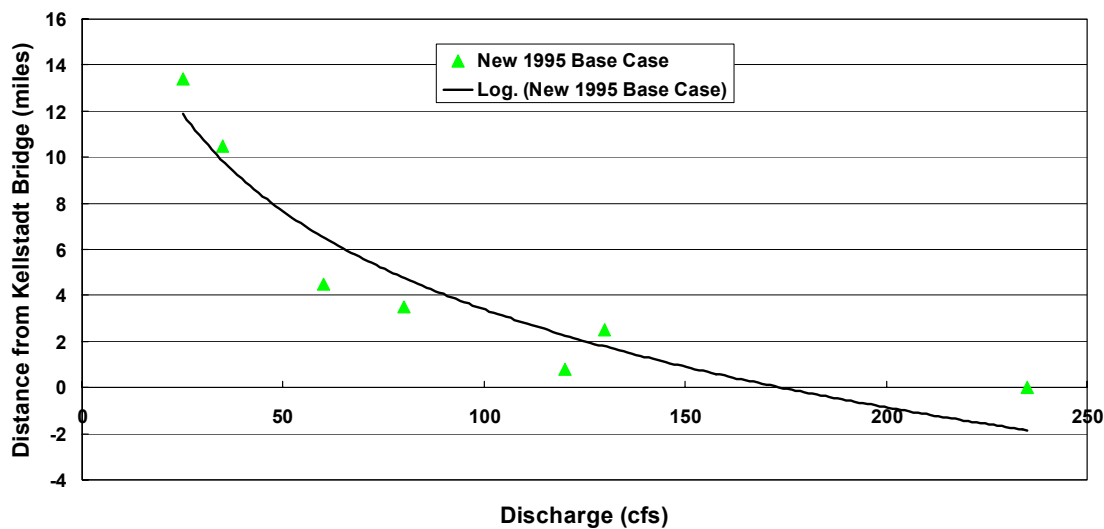


Figure F-14. Location of the 5-ppt Isohaline Zone in the 1995 Base Case Simulation

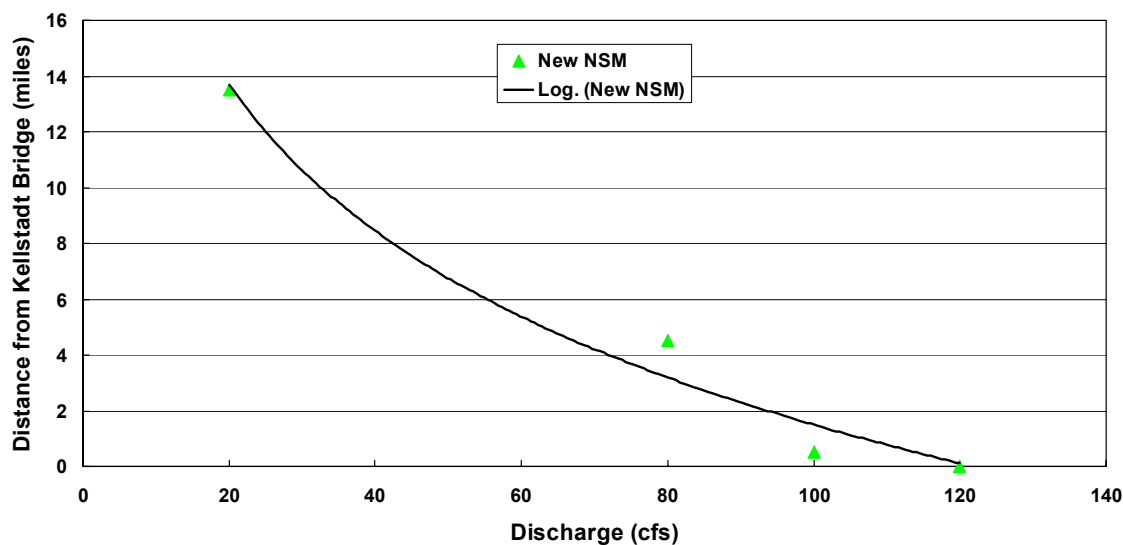


Figure F-15. Location of the 5-ppt Isohaline Zone for the NSM Simulation

According to the prediction results, the relationship between the location of the 5-ppt isohaline zone and the discharge rate can be described as follows:

$$L = -6.1 \ln(Q_f) + 33.1 \quad \text{1995 Base Case}$$

$$L = -7.6 \ln(Q_f) + 37.9 \quad \text{NSM}$$

When discharge is larger than 175 cfs for the 1995 Base Case, the 5-ppt isohaline zone is downstream of Kellstadt Bridge on the North Fork of the St. Lucie River.

Summary

The hydrodynamic and salinity simulations used to determine and monitor MFLs can be further improved with more accurate inflow and bathymetry data. For the most part, a three-dimensional model will work best. Prediction of the location of the 5-ppt isohaline zone for the North Fork should be conducted with a two-dimensional RMA model.

